Analyst

COMMUNICATION

View Article Online
View Journal

Cite this: DOI: 10.1039/d5an01298h

Received 8th December 2025,
Accepted 23rd February 2026

DOI: 10.1039/d5an01298h

rsc.li/analyst

Multimodal AFM-IR nanospectroscopy and non-linear optical microscopy for detecting collagen matrix alterations

Jérémie Mathurin,[a] Gaël Latour,[b,c] Gervaise Mosser,[d] Alexandre Dazzi,[a] Marie-Claire Schanne-Klein[b] and Ariane Deniset-Besseau*[a]

Correlative photothermal infrared nanospectroscopy (AFM-IR) and non linear optical microscopy analyses reveal that the emergence of a 1730 cm^{-1} IR band in collagen arises from local, thermally induced esterification. This band serves as a marker of irreversible molecular alteration, associated with structural destabilisation and chemical changes within the collagen matrix.

Introduction

Collagen plays an essential structural role in many connective tissues such as skin, tendon, bone, ligament, cartilage, and cornea. At least 28 different collagen types have been identified, with diverse structures, functions, and distributions. The most prevalent are types I, II, III, and IV, which can be classified as fibrillar (I, II, and III) or non-fibrillar (IV). Fibrillar type I collagen is the most abundant, providing strength, support, and elasticity to connective tissues. Each molecule is composed of three PPII-chains supercoiled into a triple helix, which self-organizes into fibrils and further into fibers. Under denaturing conditions this hierarchical organization unravels and the triple helix is lost, disrupting the amino acid spatial arrangement. Apart from enzymatic degradation, three main collagen degradation pathways are reported in the literature:[1,2] hydrolysis, oxidation and denaturation. Early steps of denaturation may be reversible, but the complete unfolding of the triple helix is irreversible and results in a fully denatured collagen, also called gelatin. A temperature increase may lead to the disruption of hydrogen bonds and intermolecular forces that maintain the protein's structure, while pH changes can disrupt electrostatic interactions. Irreversible denaturation processes, such as exposing collagenous animal tissues to high temperatures (>60 °C) for an hour or more, are characterized by the complete loss of molecular organization and the transition to gelatin. Moreover, diverse external factors, including bacterial activity leading to surface acidification, storage in humid environments, or combinations of stressors, can produce a wide range of degradation states. These processes, their origin, and their consequences are the subject of extensive investigation. Such denaturation has significant consequences not only in biomedical applications but also in cultural heritage sciences where collagen-based artifacts are concerned.[3–5]

In previous work,[3] our team demonstrated that the level of collagen degradation can be assessed using two complementary techniques: non-linear optical (NLO) microscopy and infrared nanospectroscopy (AFM-IR). NLO microscopy is a three-dimensional laser-scanning imaging technique that combines several modalities, including two-photon excited fluorescence (2PEF) and second-harmonic generation (SHG). SHG signals occur at exactly twice the excitation frequency and are characteristic of dense, non-centrosymmetric structures such as fibrillar collagens,[6–8] whereas disordered assemblies or denatured collagen loses SHG but may gain fluorescence due to chemical modifications.[3,4] This behaviour has been demonstrated in purified collagen matrices as well as in collagen-based materials as parchments by comparing well-preserved and thermally-degraded samples.[3] SHG microscopy is now a gold-standard label-free technique for collagen imaging at the submicron scale, as it is non-invasive and allows rapid imaging over around 1 mm^2 field of view.[8]

The AFM-IR technique couples the surface description capabilities of an atomic force microscopy (AFM) at the nanoscale to the analytical capability of IR spectroscopy.[9] It relies on the detection of the photo-thermal expansion that occurs within a sample after the absorption of mid-IR radiation, thanks to the AFM tip directly in contact with the analysed surface. This hybrid technique allows chemical speciation with a lateral resolution of a few tens of nanometres independently of the excitation wavenumber.[10–14] It has been used to investi-

[a]Institut de Chimie Physique, UMR 8000, Université Paris-Saclay, CNRS, 91405 Orsay, France. E-mail: ariane.deniset@universite-paris-saclay.fr
[b]Laboratoire d'Optique et Biosciences, Ecole Polytechnique, CNRS, Inserm, Institut Polytechnique de Paris, 91 120 Palaiseau, France
[c]Université Paris-Saclay, 91190 Gif-sur-Yvette, France
[d]Sorbonne Université, CNRS, Laboratoire de Chimie de la Matière Condensée de Paris, LCMCP, F-75005 Paris, France

gate individual collagen fibres extracted from parchments and localise their alteration,[3] by tracking changes of the amide I band and the appearance of an absorption band centered at around 1730 cm^{-1}. This band was not observed in well-preserved parchments even though they may contain compounds that can absorb in the same spectral range, like remaining lipids or carbonates.[15,16] It appeared in the presence of what was described as altered collagen,[17] and assumed to be linked to the oxidation of the polypeptidic chains, resulting in a loss of SHG signal and an increase of endogenous fluorescence signal. The degradation processes responsible for the onset of the 1730 cm^{-1} absorption band nevertheless remain unclear and probably depend on environmental and historical factors.[1] Beyond heritage and model collagen materials, a spectral feature in the 1730–1740 cm^{-1} region has also been reported in mechanically loaded ligament tissues and interpreted as an indicator of collagen damage or molecular unraveling.[18,19] In these studies, the emergence of this band has been correlated with mechanical fatigue, hydration–dehydration cycles, local mechanical changes, or alterations in collagen autofluorescence, without addressing its chemical origin. While these works demonstrate the relevance of the ~1730 cm^{-1} band as an empirical marker of collagen alteration in complex biological environments, they highlight the need for simplified model systems and chemically specific approaches to clarify its molecular assignment.

As we proposed in a previous study[3] the 1730 cm^{-1} band as a potential marker of fibrillar collagen alteration, it was essential to clarify its origin. Several complementary approaches have been proposed to detect collagen triple-helix denaturation, including fluorescent labeled collagen hybridizing peptides.[20,21]

While highly effective for identifying unfolded collagen in biological tissues, such probes provide limited information on the chemical nature of the alteration and rely on exogenous labeling. In the present work, we deliberately adopt a label-free strategy combining infrared nanospectroscopy and NLO microscopy, to directly probe molecular structure and chemical functionalities, an approach particularly suited to model collagen materials and heritage materials.

Local thermal degradation of collagen has previously been induced using a Wollaston wire.[22] In our study, we employed a comparable setup based on a modified AFM tip equipped with a thermocouple at its apex, integrated into the AFM system used for IR analysis. AFM-IR and NLO microscopy measurements were initially conducted at the micrometer scale on model collagen matrices prepared from purified type I collagen, to investigate fibrillar collagen organization. To further characterize the molecular state, the same approach was then applied to isolated type I collagen fibrils.

Materials and methods

Collagen samples

For this study, two types of preparations based on fibrillar type I collagen were used. One of the conditions allowed the formation of fibrillar collagen gels (hereafter referred to as C-GELs), which were ideal for FTIR and AFM-IR measurements aimed at analysing the overall response of altered fibrillar collagen.

The other preparation condition resulted in a loose collagen fibrillar networks (referred C-LFNs), suitable for localized and correlative analyses combining Second Harmonic Generation (SHG) microscopy and AFM-IR spectroscopy.

For both samples, type I collagen was purified from rat tail tendon and solubilized in 500 mM acetic acid.[23]

5 mg ml^{-1} and 1 mg ml^{-1} acidic collagen solutions were used respectively for the 5 mg ml^{-1} gel (C-GELs) and the 1 mg ml^{-1} loose fibrillar network (C-LFNs). Fibrillogenesis was achieved by submitting both solutions under ammonia vapor for 24 h or 1 h respectively for C-GELs and C-LFN. C-GEL and C-LFN were rinsed several times with distilled water. C-LFNs in water were vortexed and a drop of this solution was deposited either on a ZnSe or on a CaF_2 coverslip and dried under a flow of dried air at room temperature. All samples were dried before measurement to ensure compatibility with infrared analysis.

Collagen alteration

Collagen has been both altered at the global scale (FTIR analysis) and at the local scale (AFM-IR and SHG measurement).

For the alteration at the global scale, samples deposited on ZnSe coverslips have been dried then heated at around 100 °C with different atmospheres (water, acetic acid at 30% and ethanol) during 1 h.

Heat denaturation at the nanoscale was induced using a nanoTA setup from NanoIR1 system (Bruker/Anasys Instrument). In this setup, a thermocouple is placed on an AFM tip (AppNano, EX-AN2-300). By tuning the voltage in this thermocouple, it is possible to heat the sample below the tip at a given temperature. The calibration to convert voltage in heating temperature is done using standard samples made of three different polymers (PU/PE/PET) which melting temperatures are perfectly known. For thermal denaturation of the collagen, the temperature was set to 350 °C at the tip apex. This temperature refers to a nominal value rather than the actual temperature reached within the sample. Heat is transferred from the tip to the sample surface, dissipated into the surrounding air, and conducted through the sample to the substrate, which acts as a heat sink. As a result, the thinner the sample, the lower the internal temperature achieved. By setting the tip's nominal temperature to 350 °C, we ensured that the local temperature in all conditions exceeded 100 °C—sufficient to induce thermal total degradation of collagen. Using the optical camera and the AFM surface description capabilities, it is possible to localise a suitable part of the sample with known thickness before the thermal denaturation or localise an area already studied with AFM-IR.

FTIR measurements

FTIR analyses were performed using a vertex 70 IR spectrophotometer (Bruker) in transmission mode with a MCT detec-

tor, nitrogen cooled. The sample was deposited on ZnSe optically polished slides. The spectral range of acquisition was 4000–600 cm^{-1}, with a 4 cm^{-1} resolution and averaging over 128 scans.

AFM-IR measurements

AFM-IR measurements on C-GELs were performed on a NanoIR 1 system (Bruker Nano/Anasys Instrument) with a bottom-up illumination through a ZnSe Prism. The other AFM-IR measurements were performed with a NanoIR2 system (Bruker Nano/Anasys Instrument) with a top-down illumination. In both cases, they were coupled to a multi-chip quantum cascade laser (QCL) source (MIRcat, Daylight Solutions; tunable repetition rate range of 0–2 MHz; spectral resolution of 1 cm^{-1}) that covered part of the mid-IR range from 1350 cm^{-1} to 1900 cm^{-1}. The AFM mode used was the contact mode using an AFM probe with spring constant of 0,03 N m^{-1} (micromash HQ:CSC38/Cr Au). This AFM probe was gold coated to avoid artefacts due to the IR absorption of silicon.

Thanks to the pulsed tunable laser, it was possible to acquire either IR absorption map at one given wavenumber (simultaneously with the corresponding topography) or local spectra. The IR absorption map have been obtained with a scan rate of 0.3 Hz and a step size varying between 30 nm and 50 nm. The local spectra were acquired with a 1 cm^{-1} spectral resolution, and at least four replicates per point were measured and co-averaged.

Data processing

AFM topography and IR absorption maps were processed using MountainsLab V9 software (Digital Surf). For each dataset, topography maps were flattened before further analysis. Colocalization of IR absorption maps was performed based on the corresponding AFM topography using the software's built-in alignment algorithm.

AFM-IR local spectra were automatically background-corrected during acquisition by the instrument software, while QCL chip discontinuities were corrected post-acquisition using a custom Python script in which a gain factor is applied by taking in account several datapoints for each chip around the break. Standard pre-processing of the AFM-IR spectra was then carried out using the open-source Quasar software, applying a Savitzky–Golay filter (third-order polynomial, 15-point window) followed by vector normalization.

NLO microscopy

NLO imaging was performed on a custom-built laser-scanning upright microscope as previously described.[3,4] A femtosecond Ti:Sa laser (Mai Tai, Spectra-Physics) tuned to 860 nm was focused on the sample using a 20× air objective with 0.8 numerical aperture (Plan-Apochromat, Zeiss). A resin cap with a 5 mm diameter glass coverslip on its top was mounted on this coverslip-corrected objective to achieve the best possible resolution: 0.6 μm in the lateral direction and 1.85 μm in the axial direction.[4] Laser power at the objective focus was around 20 mW. We verified that the multiphoton signals did not decrease upon sequential imaging of the same region of interest, indicating the absence of any observable damage in the studied samples. The 2PEF and SHG signals were detected in two parallel channels in the forward direction using suitable spectral filters (FF01-720/SP and FF01-680/SP from Semrock, and GG455 from Schott for the 2PEF signal and FF01-720/SP, FF01-680/SP and FF01-427/10 from Semrock for the SHG signal) and photon-counting photomultiplier tubes (P25PC, Sentech). Image stacks were recorded at 200 kHz pixel rate, with 115 nm pixel size and 1 μm axial steps. Images were processed using Fiji to display images in false colors: SHG signals in green and 2PEF signals in red.

Multimodal correlative measurements

The correlation between images acquired by NLO microscopy and AFM-IR measurements was ensured by the following protocol: (i) NLO microscopy of the C-LFNs deposited on a coverslip to localize areas of interest for AFM-IR identified as regions where the collagen thickness-measured using the SHG signal – is around a few hundreds of nanometers, (ii) AFM-IR measurements before and after C-LFNs denaturation, (iii) NLO microscopy on the very same areas as those previously characterized. This correlative approach has been performed on 4 samples.

To ensure optimal colocalization of the regions of interest, we first compared the low-magnification images acquired by NLO microscopy with the optical images from the NanoIR2 system to achieve a global alignment. We then compared the high-magnification NLO images with large-area AFM topography maps (80 μm × 80 μm) to obtain precise colocalization.

Results and discussion

IR signature of intact and altered type I C-GELs

Vibrational spectroscopies, and particularly IR spectroscopy, are powerful tools to study protein secondary structure. Typical IR absorption spectra of proteins exhibit nine characteristic vibrational modes of the peptide bond.[24] The most prominent ones include the amide I band centered at around 1650 cm^{-1} (mainly due to C=O stretching), amide II at around 1540 cm^{-1} (N–H bending and C–N stretching), amide III at around 1230 cm^{-1} (N–H bending, C–N and C–C stretching), as well as amide A and amide B at around 3300 cm^{-1} and 3100 cm^{-1}, respectively. Among these, the most intense and informative is the amide I band, which is widely used to study secondary structure. The amide I band originates from the vibrations of backbone carbonyl groups and is sensitive to hydrogen-bonding patterns, dipole–dipole interactions, and the conformational geometry of the polypeptide chain. Its complex contour arises from overlapping components corresponding to typical secondary structures such as α-helices, β-sheets, turns, or irregular structures. This complexity is further related to differences in the intrinsic basicity of backbone carbonyls and by variations in hydrogen-bonding strength: strong hydrogen

bonds lengthen the C=O bond and lower its vibrational frequency, shifting absorption to lower wavenumbers. Although coupling between similar carbonyl stretching modes cannot be excluded, the heterogeneity of carbonyl environments—particularly those of Gly-X-Y triplet residues in the collagen triple helix—is considered the main factor underlying the different amide I profiles of collagen and gelatin molecules.[25] From the literature,[25] deconvolved spectra consistently reveal three amide I components at 1660, 1643, and 1633 cm^{-1} in native, denatured and/or partially folded collagen. The relative intensities of these peaks vary with the degree of collagen folding and triple-helix content, demonstrating their conformational dependence. Although precise one-to-one assignments are not feasible in such a complex protein, the 1660 cm^{-1} band is generally associated with helix-related hydrogen-bonded carbonyls. Interestingly, in the denatured state of the collagen molecule (*i.e.* gelatin) an enhancement of the 1633 cm^{-1} band (contribution of the intrachain H-bond) and a depletion of the 1660 cm^{-1} band is observed.[25]

In fibrils, these molecules adopt a quarter-staggered alignment stabilized by intermolecular hydrogen bonds and covalent crosslinks, giving rise to the characteristic 67 nm D-banding pattern. The amide I band of intact C-GEL (dashed dot spectrum in Fig. 1) is consistent with the spectrum of fibrillar collagen reported in the literature[26] (to be distinguished from the collagen molecule) and can be described as a superposition of three sub-bands: a main one centered around 1665 cm^{-1} and two shoulders around 1630 and 1690 cm^{-1}. These three sub-bands are generally attributed to the presence of intra- and inter-molecular hydrogen bonds, which are the cause of the three non-equivalent carbonyls bonds in the molecule. The main peak around 1665 cm^{-1} is attributed to the carbonyl of the backbone structure of the triple helix.[27] The two side shoulders at 1630 cm^{-1} and 1690 cm^{-1} are associated respectively to intramolecular hydrogen bonds (either between PPII chains or with incorporated water) of carbonyl bond[25] and to intermolecular hydrogen bonds. As a consequence, variation of the bands profile in terms of intensity and position can be a good indicator of structural changes of fibrillar type I collagen due to physico-chemical modifications. To highlight the IR signature of altered collagen fibrils, a global FTIR study was led on C-Gels after heating under different atmospheres. Due to technical limitations of our setup, it was not possible to heat C-GELs above 100 °C. After heating the C-Gels at 75 °C for 1 h, the amide I band showed different spectral variations. Under a humid (water) atmosphere (blue spectrum in Fig. 1), a broadening of the band was observed with an increase of the two-sided shoulders at 1695 and 1630 cm^{-1}, associated with, respectively, a weakening of the intermolecular hydrogen bonds[28] and a replacement of some intramolecular hydrogen bonds between carbonyl groups and adjacent NH group by a hydrogen bond with water (shift of amide bond to higher frequency). The first one signed a decrease of cohesion between adjacent collagen molecules and consequently the destabilization of the fibrillar organization, while the second one signed the destabilization of the triple helix. When exposed to ethanol vapors (red spectrum in Fig. 1), the amide I broadening was more pronounced at higher frequencies. The literature[29] description of the impact of ethanol on the structure of collagen gels shows that ethanol tends to replace water in water-mediated hydrogen bonds, decreasing the number of intramolecular hydrogen bonds, which are important for fibril organization, while not affecting other hydrogen bonds. In both cases, the 1730 cm^{-1} band was absent, showing that loss of organization alone does not explain its appearance.

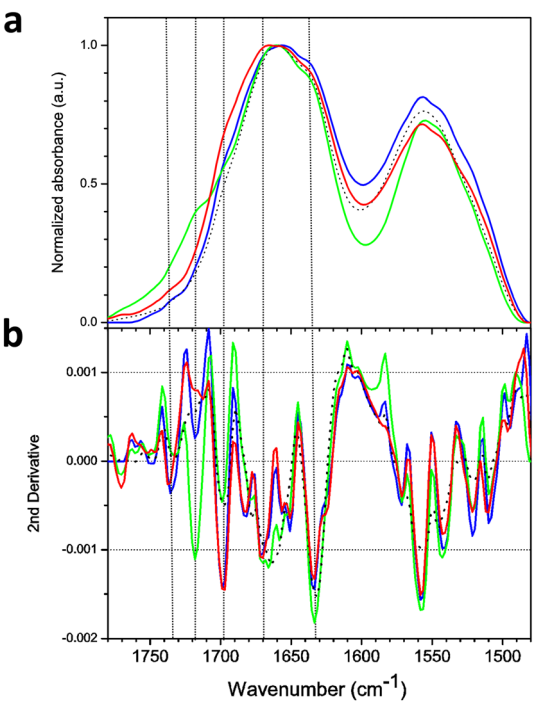

Fig. 1 FTIR analysis of the amide I and II bands and the ester absorption area of type I C-GELs in their native state (dashed black line) or after thermal alteration under different atmospheres: 100% humidity (blue), ethanol vapour (red) and acidic vapour using a heated 30% acetic acid solution (green). (a) FTIR spectra. (b) Second derivative of the same spectra.

Under acetic acid vapor (green curve in Fig. 1), the amide I band broadening occurred together with the appearance of a new shoulder at 1718 cm^{-1}. In light of the chemical structures of collagen and acetic acid, we suspect either a direct adsorption of acetic acid and/or a potential esterification reaction between the carboxylic group of acetic acid and the accessible hydroxyl groups of hydroxyproline residues. As the IR response of acetic acid can be strong compared to a potential ester bond formation, this global analysis is inconclusive and reinforces the need for local analysis. In the case of ester bond formation, this hypothesis might be supported by the observation that heating appears to induce a reorganization of hydrogen bonds within the C-GELs. This reaction may occur if heating renders hydroxyproline groups accessible for intra- and/or inter-molecular esterification with neighbouring carboxylic groups. The detection of this band might be an indicator of the thermal

history of collagen-based samples. Furthermore, the esterification reaction necessitates the presence of at least water molecules in the sample surroundings. If observed, this event will induce a potential irreversible degradation of the fibrillar type I collagen structure. To verify this assumption, local alterations were performed directly on C-GELs.

Impact of local heating on C-GELs

To explore the impact of thermal alteration, a local heating gradient was induced at the surface of a C-GEL (Fig. 2a) with a thermocouple disposed on an AFM tip (nanoTA). The temperature of the nanoTA tip was set at the maximum (350 °C) to alter the matrix to a few microns depth.[22] During the heating step, the nanoTA tip was moved so that the altered area appeared as an hourglass on the optical image (Fig. 2a). The close vicinity seemed intact. The procedure allowed the investigation of both intact and heated areas. The studied area (yellow rectangle Fig. 2a) exhibited a chaotic topography (Fig. 2b) with a sharp border (right corner on the height image – a few microns deep). A series of spectra along a line (coloured crosses Fig. 2b – spectra Fig. 2c) was acquired next to the border using the same AFM with the AFM-IR modality. Far from the heated area, the amide I band (purple and deep blue spectra) exhibits a similar shape as the native fibrillar collagen I with a maximum absorption centered at 1660 cm^{-1} and two shoulders at around 1630 cm^{-1} and 1690 cm^{-1}.[25] Getting closer to the heated area, a clear broadening of the amide I band was observed together with the raising of the 1720 cm^{-1} band (yellow to red spectra Fig. 2c). The results are akin to the FTIR analysis: the amide I band broadening is characteristic of the general weakening of the hydrogen bond network, generating the destabilization of the fibrillar organization as well as the triple helix of the collagen molecule.[25] Furthermore, the band centred around 1720 cm^{-1}, highlighted a potential irreversible alteration of the collagen molecule. Next to the sharp border (wine-color, grey and black curves), the broadening of the amide I band was extreme; it looks like a band-continuum that might indicate a total loss of collagen triple helices and their transformation into gelatin.

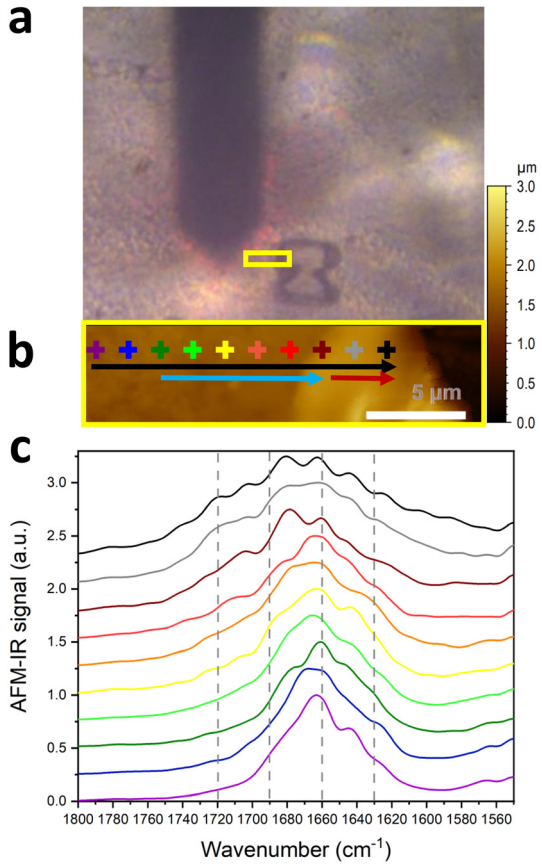

Fig. 2 Thermal alteration of a C-GEL sample. (a) Optical image of the sample surface after thermal alteration using a nanoTA tip; the hourglass pattern left to the cantilever corresponds to the area where the collagen was burned. (b) AFM topography obtained on the area localized with a yellow rectangle on the optical image. (c) Series of spectra recorded along the line marked on the AFM topography; the colour gradient corresponds to the position of the spectrum relative to the heated area (purple non-heated to black the closest of the burned area); the blue arrow on AFM topography corresponds to the area in which changes are observed on the amide I band but the general shape is still conserved, the red arrow corresponds to the area in which the amide I band is too broad, corresponding to highly altered areas.

Compared to FTIR analysis for which the 1730 cm^{-1} band was only observed in the presence of acetic acid, here this band was detected, whereas only water was in the close vicinity of the fibrils. This confirms that a potential irreversible chemical alteration can be induced in C-GELs without any acidic or oxidative environment[1] and without molecules that naturally co-exist in collagenic tissues.[30] In other words, thermal processes by themself seem to be sufficient to generate a possible esterification of the destabilized collagen molecule with the appearance of the ester-carbonyl band around 1730 cm^{-1}.

Furthermore, the AFM-IR study highlights the existence of an alteration continuum or, at least, several degrees of alteration that might be assigned through amide I band structure. To confirm the link between the shape of the amide I band and the degree of fibrils alteration or the destabilization of the collagen triple helix, complementary SHG measurements were performed. SHG signals are expected from well-preserved fibrillar collagen whereas these signals disappear when the hierarchical structure of collagen is lost. This non-contact technique complements local IR signals by probing the fibrillar structure of collagen.

Multimodal analysis of C-LFNs

To pinpoint local alterations and differentiate fibril destabilization from the loss of secondary structure in collagen molecules, the same heating procedure was applied to collagen fibrils isolated from a C-LFN deposited on CaF_2 slides. Fig. 3a shows a typical AFM topography of a fibril assembly in contact mode.

The assembly is composed of fibrils about 50 nm thick, as shown in the thickness histogram of Fig. 3a. These fibrils are either distributed individually or stacked (left part of the assembly). Unfortunately, due to the sample softness, border effects were observed (right side of the assembly) where the IR

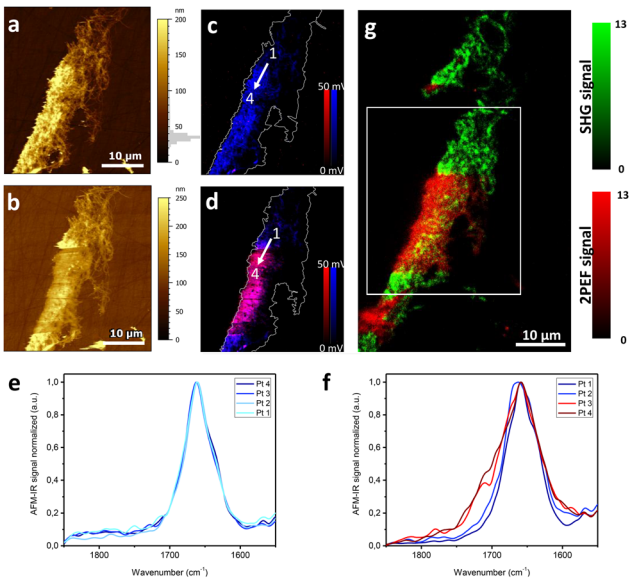

Fig. 3 Thermal alteration of collagen fibrils. (a) and (b) AFM topography obtained on the area before (a) and after (b) thermal alteration. The histogram of fibrils thickness is plotted on the thickness scale in (a). (c) and (d) Composite images obtained by overlaying IR mapping at 1660 cm^{-1} (in blue) and at 1725 cm^{-1} (in red). (e) Multiphoton microscopy image of the collagen fibrils after thermal alteration, the white square corresponds to the area previously analysed using AFM-IR: merging of SHG signal (in green) and endogenous 2PEF signal (in red). The color bars indicate the number of collected photons in every channel. Regions with both signals appear in yellow. (f) and (g) Local IR absorption spectra obtained along the lines indicated in (c) and (d).

signal dropped. The IR spectra acquired along the white line (indicated by the white arrow in Fig. 3c) showed an amide I band similar to that of non-altered fibrillar type I collagen gels, without any absorption at 1725 cm^{-1}. The overlay map (Fig. 3c) of the two IR maps acquired at 1660 cm^{-1} (blue) and 1725 cm^{-1} (red) confirms the homogeneity of the assembly that only shows the 1660 cm^{-1} absorption. A square region on top of the assembly was then selectively heated using the nanoTA tip. This heated area appears in the AFM topography image (Fig. 3b) as a region of reduced thickness. Series of local spectra acquired at the same location as before heating (Fig. 3g) crossed the boundary between heated and non-heated fibrils. At the border of the heated zone, the IR spectra either maintained the same shape as before heating or showed a slight broadening of the amide I band (Fig. 3g blue curves). In contrast, inside the heated zone (Fig. 3g red and dark red curves), the IR spectra exhibited a pronounced broadening of the amide I band and a shoulder at 1725 cm^{-1}, indicating both a structural change and a possible irreversible chemical modification. On the composite image (Fig. 3d), an intense signal appeared at 1725 cm^{-1} where the sample has been heated.

The SHG-2PEF measurements confirmed the structural and chemical changes. Fig. 3e presents the overlay of the endogenous 2PEF signal of the collagen (red) and its SHG signal (green). Inside the heated zone, 2PEF signal increased whereas the SHG signal decreased. A decrease in the SHG signal indicates a loss of hierarchical fibrillar organization—from the fiber to the fibrils and, ultimately, to the collagen molecule itself—which is revealed by IR analysis as a progressive broadening of the amide I band. In contrast, an increase in 2PEF signal suggests a drastic change in chemical composition, consistent with the appearance of the 1730 cm^{-1} band in the IR absorption spectrum. At this scale, heating the type I collagen fibril generated a local potential irreversible alteration of the collagen molecules confirmed by both AFM-IR and NLO measurements.

To clarify this mechanism, a single fibril from a C-LFN sample was studied by AFM-IR before and after heating. The studied fibril (Fig. 4a) was around 20 nm in height, as

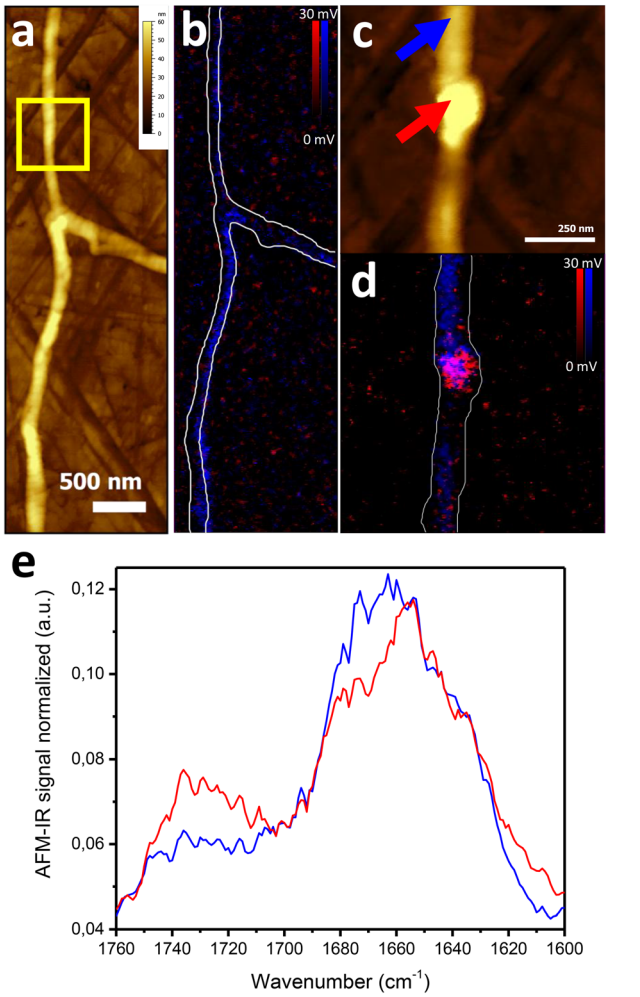

Fig. 4 Thermal alteration of a single collagen fibril. (a) AFM topography of the region prior to thermal treatment; (b) composite IR map showing absorbance at 1660 cm^{-1} (blue) and 1725 cm^{-1} (red) of the fibril before thermal treatment; (c) AFM topography acquired after thermal alteration, corresponding to the yellow square highlighted in panel (a); (d) composite IR map showing absorbance at 1660 cm^{-1} (blue) and 1725 cm^{-1} (red) of the fibril after thermal treatment (e) IR spectra recorded at the positions indicated by the colored arrows, showing a comparison between a non-heated region (blue) and the globular structure formed after localized heating (red).

expected.[31] After heating, a morphological change was observed, with local thermal alteration leading to the formation of a globule and a depletion of surrounding material (Fig. 4c). The globule showed an absorption at 1725 cm^{-1}, indicating a local chemical alteration caused by the heating process (Fig. 4d), as confirmed by the local spectra (Fig. 4e) showing a 5 cm^{-1} shift of the maximum of absorption. In the outer region of the globule, spectra resembled that of type I collagen.

In fibrils or gels studied using AFM-IR, the only available carboxylic acid groups able to interact with hydroxyproline originate from amino acids located at strand ends or released during the early stages of degradation, mainly glutamic (≈5%) and aspartic (≈3%) acids.

Furthermore, literature reports thermolabile domains near the C-terminal region of the collagen molecule,[32] where heating can partially open the triple helix and expose acidic residues. These domains, representing up to 9% of the amino acids, could similarly promote ester formation with hydroxyproline, predominantly at the fibril periphery. Such reactions are expected to occur mainly within the uppermost layers of the sample, to which AFM-IR is more sensitive, explaining the stronger carbonyl IR signal observed in AFM-IR compared with conventional FTIR. This mechanism could account for the presence of the 1730 cm^{-1} band in pure fibrillar collagen only when the temperature is sufficiently high to induce molecular degradation. In more complex environments, such as parchment, the hydroxyl reactive sites may instead interact with carboxylic acid-rich species—such as lipids or ink components[33]—allowing ester formation at lower temperatures, without the need to thermally degrade the collagen molecule to generate carboxylic groups.

Conclusion

We conducted a multiscale multimodal analysis of thermally altered type I collagen gel to elucidate the appearance in the IR spectra of a 1730 cm^{-1} band when looking at altered old parchments at the nanoscale. This process might intervene in two steps. First, a structural change of the type I collagen fibril structure related to the weakening of intra and inter-molecular hydrogen bonds. Then, the hydroxyl part of hydroxyproline, which is no longer involved in hydrogen bonds, can react with any carboxylic acid function which is present in the vicinity. If the first step can potentially be reversible, the second one is not due to the steric hindrance generated by chemical modification. Thus, the 1730 cm^{-1} band is a possible marker of irreversible alteration of collagen fibrils. Depending on the surrounding medium, the appearance of the 1730 cm^{-1} absorption band is more or less pronounced. In a complex medium such as parchments, in which many molecules with terminal carboxylic acid can be found, it can easily occur. However, for a pure type I fibrillar collagen matrix, the collagen molecule must be degraded, and the amide bonds broken to release carboxylic acid donors into the medium.

Author contributions

J. M. conceptualization, investigation, methodology, validation, formal analysis, visualization, writing – original draft, writing – review and editing. G. L. investigation, formal analysis, visualization, and review. G. M. resources, validation and review. A. D. investigation, validation, and funding. M.-C. S.-K. validation, funding and review. A. D.-B. investigation, validation, formal analysis, project administration, visualization, writing – original draft, writing – review and editing.

Conflicts of interest

There are no conflicts to declare.

Data availability

Data for this article (FTIR, AFM-IR and SHG measurements) are available at [Multimodal AFM-IR Nanospectroscopy and Non-Linear Optical Microscopy for Detecting Collagen Matrix Alterations – Dataset] at [https://zenodo.org/records/17790594].

Acknowledgements

The authors acknowledge funding from Paris-Saclay IDEX (11-IDEX-0003) and from CNRS (MITI, DEFI Imag'In). GL and MCSK acknowledge funding from Agence Nationale de la Recherche (ANR-10-INBS-04, ANR-11-EQPX-0029). The authors thank L. Robinet for the discussions around the project.

References

1 C. J. Kennedy and T. J. Wess, *Restaurator*, 2003, **24**, 61–80.
2 K. Müller, Z. Szikszai, Á. Csepregi, R. Huszánk, Z. Kertész and I. Reiche, *Sci. Rep.*, 2022, **12**, 113.
3 G. Latour, L. Robinet, A. Dazzi, F. Portier, A. Deniset-Besseau and M.-C. Schanne-Klein, *Sci. Rep.*, 2016, **6**, 26344.
4 M. Schmeltz, L. Robinet, S. Heu-Thao, J.-M. Sintès, C. Teulon, G. Ducourthial, P. Mahou, M.-C. Schanne-Klein and G. Latour, *Sci. Adv.*, 2021, **7**, 1090–1106.
5 K. M. Axelsson, R. Larsen, D. V. P. Sommer and R. Melin, *Stud. Conserv.*, 2016, **61**, 46–57.
6 W. R. Zipfel, R. M. Williams, R. Christiet, A. Y. Nikitin, B. T. Hyman and W. W. Webb, *Proc. Natl. Acad. Sci. U. S. A.*, 2003, **100**, 7075–7080.
7 X. Chen, O. Nadiarynkh, S. Plotnikov and P. J. Campagnola, *Nat. Protoc.*, 2012, **7**, 654–669.
8 S. Bancelin, C. Aimé, I. Gusachenko, L. Kowalczuk, G. Latour, T. Coradin and M.-C. Schanne-Klein, *Nat. Commun.*, 2014, **5**, 4920.
9 A. Dazzi and C. B. Prater, *Chem. Rev.*, 2017, **117**, 5146–5173.

10 V. Giliberti, M. Badioli, A. Nucara, P. Calvani, E. Ritter, L. Puskar, E. F. Aziz, P. Hegemann, U. Schade, M. Ortolani and L. Baldassarre, *Small*, 2017, **13**, 1701181.
11 F. S. Ruggeri, S. Vieweg, U. Cendrowska, G. Longo, A. Chiki, H. A. Lashuel and G. Dietler, *Sci. Rep.*, 2016, **6**, 1–11.
12 J. Waeytens, J. Mathurin, A. Deniset-Besseau, V. Arluison, L. Bousset, H. Rezaei, V. Raussens and A. Dazzi, *Analyst*, 2021, **146**, 132–145.
13 F. Lu and M. A. Belkin, *Opt. Express*, 2011, **19**, 19942.
14 F. Lu, M. Jin and M. A. Belkin, *Nat. Photonics*, 2014, **8**, 307–312.
15 L. Gonzalez and T. Wess, *Appl. Spectrosc.*, 2008, **62**, 1108–1114.
16 M. Odlyha, C. Theodorakopoulos, J. De Groot, L. Bozec, M. Horton and M. Schreiner, *e-Preserv. Sci.*, 2009, **6**, 138–144.
17 M. Derrick, *J. Am. Inst. Conserv.*, 1991, **10**, 49–65.
18 K. H. Putera, J. Kim, S. Y. Baek, S. H. Schlecht, M. L. Beaulieu, V. Haritos, E. M. Arruda, J. A. Ashton-Miller, E. M. Wojtys and M. M. Banaszak Holl, *Commun. Biol.*, 2023, **6**, 564.
19 J. Chen, J. Kim, W. Shao, S. H. Schlecht, S. Y. Baek, A. K. Jones, T. Ahn, J. A. Ashton-Miller, M. M. Banaszak Holl and E. M. Wojtys, *Am. J. Sports Med.*, 2019, **47**, 2067–2076.
20 J. Kim, S. Y. Baek, S. H. Schlecht, M. L. Beaulieu, L. Bussau, J. Chen, J. A. Ashton-Miller, E. M. Wojtys and M. M. Banaszak Holl, *J. Exp. Orthop.*, 2022, **9**, 74.
21 J. L. Zitnay, Y. Li, Z. Qin, B. H. San, B. Depalle, S. P. Reese, M. J. Buehler, S. M. Yu and J. A. Weiss, *Nat. Commun.*, 2017, **8**, 14913.
22 L. Bozec and M. Odlyha, *Biophys. J.*, 2011, **101**, 228–236.
23 F. Gobeaux, E. Belamie, G. Mosser, P. Davidson, P. Panine and M. M. Giraud-Guille, *Langmuir*, 2007, **23**, 6411–6417.
24 A. Barth, *Biochim. Biophys. Acta, Bioenerg.*, 2007, **1767**, 1073–1101.
25 K. J. Payne and A. Veis, *Biopolymers*, 1988, **27**, 1749–1760.
26 I. V. Yannas, *J. Macromol. Chem.*, 1972, **7**, 49–106.
27 B. B. Doyle, E. R. Blout and E. G. Bendit, *Biopolymers*, 1975, **14**, 937–957.
28 G. Shanmugam and P. L. Polavarapu, *Chirality*, 2009, **21**, 152–159.
29 A. Gopinath, S. M. M. Reddy, B. Madhan, G. Shanmguam and J. R. Rao, *Eur. Biophys. J.*, 2014, **43**, 643–652.
30 L. Gonzalez, M. Wade, N. Bell, K. Thomas and T. Wess, *Appl. Spectrosc.*, 2013, **67**, 158–162.
31 D. R. Baselt, J. P. Revel and J. D. Baldeschwieler, *Biophys. J.*, 1993, **65**, 2644–2655.
32 C. A. Miles and A. J. Bailey, *Micron*, 2001, **32**, 325–332.
33 S. C. Boyatzis, G. Velivasaki and E. Malea, *Heritage Sci.*, 2016, **4**, 13.

